20th CIRP Conference on Electro Physical and Chemical Machining (ISEM 2020)

Development of low-cost production process for prototype components based on Wire and Arc Additive Manufacturing (WAAM)

Nataliia Chernovol[a]*, Bert Lauwers[b], Patrick Van Rymenant[c]

*a,b,c*KU Leuven, Department of Mechanical Engineering, Celestijnenlaan 300, 3001 Leuven, Belgium

* Corresponding author. Tel.: +32(0)-499-83-79-50. *E-mail address:* nataliia.chernovol@kuleuven.be

Abstract

Wire and Arc Additive Manufacturing is a fast-growing technology that allows to produce medium to large metal parts in both a material- and cost-efficient way. Because it is based on existing welding technology, it is certainly an affordable technology for small and medium sized companies. However, the integration of this technology for prototype manufacturing still needs certain difficulties to be solved, such as the determination of process parameters and deposition strategies, programming software to be used, postprocessing, etc. This paper focuses on the different steps to be taken to adapt the existing Gas Metal Arc Welding (GMAW) technology into an affordable and efficient WAAM technology. The technology developed has been integrated within a robotized platform. Experiments for the determination of bead geometry were conducted both for conventional GMAW (MAG welding) and Cold Metal Transfer (CMT) welding. A central composite rotatable design (CCD) was used for fitting second-order response surfaces, allowing to predict bead geometry corresponding to the welding parameters and to set the required information for generating the robot programs. Also, productivity of both processes was compared, highlighting significant dependency on part's geometry and dimensions as also the quantity of parts simultaneously produced.

Keywords: WAAM;GMAW;CMT;comparison;bead geometry prediction.

1. Introduction

Additive manufacturing (AM) is widely used in machine building, aerospace, medical and other industries for rapid prototyping and production of one-off parts. Compared to conventional subtractive manufacturing, it allows production of multi-metal parts and reduction of the lead-time, the amount of machining scrap and the costs involved with the part's production.

An upcoming and promising AM technique for manufacturing metal structures is Wire and Arc Additive Manufacturing (WAAM). WAAM is an AM technique that uses an electric arc as a heat source to melt a wire and build a component layer by layer. The process offers the opportunity to create large size components, has high material usage efficiency (up to >90%), relatively high deposition rates (1-4 kg/h [1] compared with wire and laser additive manufacturing

1.5-48 g/min [2]) and increased energy efficiency [2]. Moreover, WAAM offers cleaner and more environmentally friendly production in comparison with powder based technology used in Metal 3D printing, green sand casting and CNC machining [3].

There are three main technologies used for WAAM: Gas Metal Arc Welding (GMAW), Gas Tungsten Arc Welding (GTAW) and Plasma Arc Welding (PAW).

Currently GMAW is mostly used for WAAM due to its higher deposition rates, the limited cost of the equipment, the possibility to weld a wider range of materials and the perfect alignment of the filler wire with the nozzle, that simplifies programming of the motion system. Within the GMAW technology several processes exist: conventional MIG/MAG, pulsed MIG/MAG, Surface Tension Transfer (STT from Lincoln Electric), Cold Metal Transfer (CMT from Fronius), etc. CMT is more and more used in WAAM due to the low heat

input, better arc stability and the spatter free deposition. It is an advanced GMAW process, that uses a controlled current waveform to form a drop and control its growth, and a specific wire feeding mechanism to deposit a metal drop with minimal heat [4], which allows to produce components with much thinner walls than the conventional GMAW process.

In order to obtain a part with the help of wire and arc additive manufacturing, a 3D CAD model is sliced into 2.5D layers. To slice the part, the layer height should be known, which is defined by the weld bead height. This height depends on the welding parameters and is usually determined experimentally for each type of wire material and diameter. After slicing the CAD model, a deposition path is generated within each layer. Finally, a program for a robot (or another NC-controlled machine tool) is obtained and a near-net shape part is produced layer-by-layer with the help of the arc welding system. To reduce residual stresses, improve mechanical and metallurgical properties post weld heat treatment might be implemented. As the WAAM process does not allow to obtain a high dimensional accuracy and surface quality (waviness of around 500μm [1]), further post processing, like NC-milling is implemented. To generate the tool path for the postprocessing step, the WAAM component is scanned. By fitting a CAD model within the scanned component, the remaining stock is calculated and used as a basis for tool path generation for milling.

Figure 1 - General process chain of part production based on WAAM

In recent years GMAW and CMT WAAM were investigated by many universities, such as Cranfield University, TU Delft, University of Wollongong, Osaka University, etc. Nevertheless, integration of the WAAM process in small and medium sized companies for rapid prototyping or low component series production still faces certain difficulties, such as adaptation of existing equipment for AM, choice of software and welding process/equipment, determination of process parameters and postprocessing.

This paper focuses on the different steps to be taken to adapt the existing GMAW technology into an affordable WAAM technology. To compare conventional GMAW and CMT processes and highlight the factors that are important for the process selection, bead geometry was experimentally determined with further valorization and discussion.

2. Equipment and software implementations

The WAAM process is mainly used with standard welding equipment, a welding power source, with a wire feed system and a torch. The motion is usually provided by a robot, but also a classical numerically controlled machine tool (e.g. milling machine) could be used. Using a robot for WAAM offers several advantages. Many robotic welding systems are available on the market. Also, they are widely used in industry, have a large working space and can easily be adopted for AM purposes. On the other hand, integration of the GMAW

technology within a milling machine tool set-up (hybrid WAAM) allows implementation of all the process steps within a single machine, simplifying process preparation by elimination of the robot programming. By combining CNC milling with WAAM, the required height of the layers could be obtained and internal surfaces, that are hard or impossible to reach during postprocessing of the final component, could be machined.

Software tools and systems play an important role in the process preparation. Nowadays, it is possible to divide the existing software for WAAM in two main categories: stand-alone applications and plug-ins that are integrated within existing CAD/CAM software.

The stand-alone application is a software that is developed specifically for the WAAM technology, often offering more flexibility, a higher degree of automation and customization of bead modeling, slicing algorithms and deposition path generation strategies. On top of that, in some of them it is possible to implement thermal simulation and stress analysis. Commercial programs, such as NetFabb are available. Moreover, new CAM software for WAAM is developing, for example, WAAMMat (Cranfield University) and Metal XL (MX3D company). Stand-alone applications however do not always provide the functionality for robot programming, meaning that additional software for off-line robot programming is required. To post-process the printed part, all necessary operations are programmed in CAM software (for milling) to be further executed on a CNC machine.

Plug-ins for WAAM are developed and integrated in CAD/CAM software such as PowerMill, Siemens NX, SprutCAM and others. The main advantage is the ability to implement the simulation of the robot movements, detect collisions and create all necessary operations for post processing within a single software platform. The functionality, compared to stand-alone applications, is sometimes limited: mainly in the variety of deposition path strategies, automatic model preparation (including sub-volumes decomposition and determination of slicing directions), possibility to implement thermal simulation and determination of internal stress levels.

3. Bead geometry- and process parameters investigation

3.1. Bead geometry prediction

In order to generate the slice geometry and the deposition paths for part production, dimensions of the weld bead geometry are required (Figure 2 and Figure 3). Layer height is used to slice the CAD model in 2D layers. To obtain the required thickness of the final component, bead width should also be determined. Moreover, to produce solid components in multi-pass multi-layer way, the step-over value, which depends on the bead width, should be calculated. The main process parameters influencing bead geometry are shown on Figure 4.

In recent years a lot of research was devoted to weld bead modelling during WAAM. The relationships between process parameters and bead geometry are not linear and were found using methods such as factorial design, linear regression, second-order regression, Taguchi method, artificial neural networks and response surface methodology.
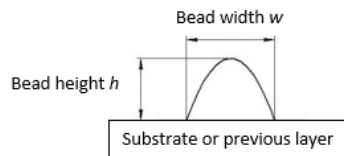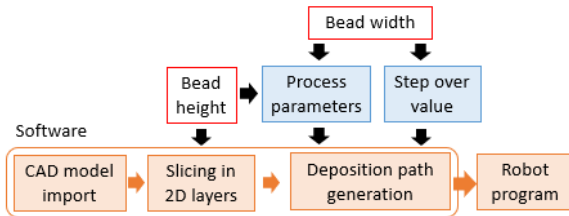
Figure 2 - Weld bead geometry

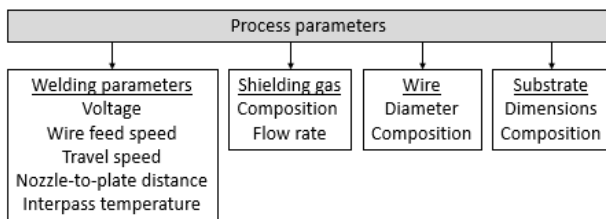Figure 3 - Generation of deposition path for WAAM

Figure 4 - Main process parameters for GMAW WAAM

Factorial design requires a large number of experiments [5]. Xiong et.al. [6] compared the neural network and second-order regression analysis and concluded that the most accurate method for bead geometry prediction is artificial neural network (max error 5.528%). Second-order regression also shows adequate results (max error 6.77%). Response surface methodology, that is described by second-order polynomial regression, shows the maximal error 7.1% [7] and could be used for bead height and width prediction.

In this study, the response surface method is used for prediction of bead geometry for two processes: conventional GMAW and CMT.

3.2. Experimental set-up

As motion system for WAAM, a CLOOS QRC320H robot cell was used. This robot cell consists of a standard industrial 6-axis robot arm and 2-axis rotary table.

To compare the conventional GMAW and CMT technology, two power sources were integrated in the robot controller: a Qineo pulse 420A machine with synergic control and a Fronius TPS 3200 CMT (Figure 5). The Qineo pulse 420A machine was integrated by the CLOOS company, and control of the welding parameters is possible directly from the program by specifying the welding lists containing information of wire feed speed, travel speed, gas pre- and post-flow, etc. The Fronius TPS 3200 CMT was integrated by our research group using a ROB 3000 robot interface. By connecting the power source to the robot digital inputs/outputs, the arc can be switched on/off directly from the robot program. Welding parameters are set only from the remote control.

Robot paths were generated using the Autodesk - PowerMill software. This CAM software has a standard library with various robot configurations and related postprocessors such as ABB, Comau, Fanuc, Mitsubishi, Kuka etc., but is lacking all CLOOS robots. To overcome the latter, the new robot cell was integrated into the robot plug-in in the PowerMill software (Figure 6).
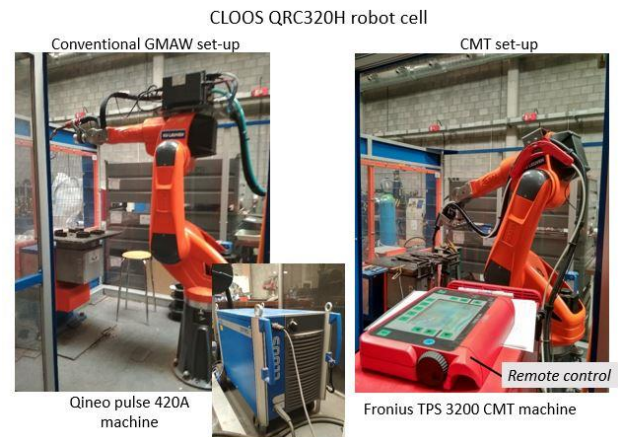

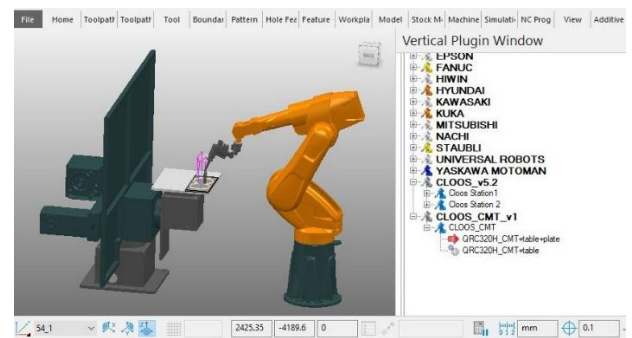Figure 5 – Experimental set-up

Figure 6 - CLOOS robot cell integrated in PowerMill robot plug-in

For bead geometry determination, the substrate plate was a mild steel plate with dimensions 30x10x200 mm. As filler material, a 1.2 mm diameter wire EN ISO 14341-A (G 42 3 M21 3Si1) was used. The shielding gas was an 85% Ar with 15% CO_2 mixture at a constant flow rate of 15 l/min. Contact tip to work distance (CTWD) was equal to 15 mm for both processes and was kept constant during deposition. During the trial runs, when the layers were deposited in one direction (zig), significant differences between the height in start and end points was observed (Figure 7). It could be explained by the temperature accumulation at the end of the weld. To eliminate the mistakes in the start/stop point, deposition direction of every second layer was reversed (zig-zag strategy). Temperature between the passes (interpass temperature) was kept below 120˚C and controlled using temperature indicator crayons.

Figure 7 - Walls printed with a) zig strategy, b) zig-zag strategy

3.3. Experimental design matrix

Input process parameters were wire feed speed (WFS) and travel speed (TS). Two response parameters were average bead height (H) and bead width (W).

A preliminary study was conducted to determine the parameters ranges. For the CMT process, TS range is narrower for lower WFS values (<2.7m/min) than for the rest of the range. For example, during WFS 1.2m/min and TS 30 cm/min humps formation was observed. Thus, to determine a bead geometry, the overall range was divided into 2 ranges.

As polynomial models give the most accurate results, Central Composite Design (CCD) was used to design the experiment. Process parameters and their limits are given in Table 1 and Table 2 for the conventional GMAW and CMT processes respectively.

Table 1. Process parameters and their limits. Conventional GMAW process

Parameters	Factor level				
	Level 1	Level 2	Level 3	Level 4	Level 5
WFS, m/min	2.5	2.9	3.8	4.6	5
TS, cm/min	15	22	38	53	60

Table 2. Process parameters and their limits. CMT process

Parameters	Factor level				
	Level 1	Level 2	Level 3	Level 4	Level 5
	Range 1				
WFS, m/min	1.2	1.4	1.9	2.5	2.7
TS, cm/min	8	11	18	25	28
	Range 2				
WFS, m/min	2.7	3.2	4.4	5.5	6
TS, cm/min	10	15	28	40	45

For every parameter set 3 replicates were produced. Every bead height was measured in three points, away from the start and end of the deposition track. Bead width measurements were performed using a digital optical microscope. As a response, average values were used both for bead width and height. Experimental design matrices and responses for conventional GMAW and CMT processes are shown in Table 3, Table 4 and Table 5.

3.4. Second-order regression models

To determine the relationships between welding parameters and bead geometry, a second order model was used as described in equation 1 [8, p. 415].

$$Y = \beta_0 + \sum_{i=1}^{k} \beta_i x_i + \sum_{i=1}^{k} \beta_{ii} x_i^2 + \sum_{i<j} \sum \beta_{ij} x_i x_j + \epsilon \qquad (1)$$

The second-order models for bead height and bead width determination for the conventional GMAW process were determined as follow:

$$H = 2.439 + 0.3348 \cdot WFS - 0.07019 \cdot TS$$
$$-0.0242 \cdot WFS^2 + 0.00062 \cdot TS^2 \qquad (2)$$
$$W = 5.37 + 3.006 \cdot WFS - 0.2145 \cdot TS - 0.1255 \cdot WFS^2$$
$$+0.002364 \cdot TS^2 - 0.02318 \cdot WFS \cdot TS \qquad (3)$$

Table 3. Experimental design matrix and responses. Conventional GMAW process.

N	WFS (m/min)	TS (cm/min)	H (mm)	W (mm)
1	2.9	22	1.913	7.729
2	4.6	22	2.236	10.406
3	2.9	53	1.260	4.803
4	4.6	53	1.504	6.302
5	2.5	38	1.389	5.256
6	5	38	1.750	8.131
7	3.8	15	2.499	11.262
8	3.8	60	1.370	5.156
9	3.8	38	1.626	6.928
10	3.8	38	1.609	6.991
11	3.8	38	1.586	6.859
12	3.8	38	1.591	6.879
13	3.8	38	1.609	6.818

Table 4. Experimental design matrix and responses. CMT process, range 1.

N	WFS (m/min)	TS (cm/min)	H (mm)	W (mm)
1	1.2	18	1.284	2.913
2	1.4	11	1.554	4.193
3	1.4	25	1.115	2.951
4	1.9	8	1.943	6.305
5	1.9	18	1.420	4.338
6	1.9	18	1.418	4.490
7	1.9	18	1.422	4.372
8	1.9	18	1.430	4.463
9	1.9	18	1.422	4.463
10	1.9	28	1.169	3.573
11	2.5	25	1.333	4.637
12	2.5	11	1.978	6.484
13	2.7	18	1.577	5.494

Table 5. Experimental design matrix and responses. CMT process, range 2.

N	WFS (m/min)	TS (cm/min)	H (mm)	W (mm)
1	2.7	28	1.453	4.089
2	3.2	15	2.121	6.097
3	3.2	40	1.427	3.740
4	4.4	10	2.904	8.147
5	4.4	28	1.773	5.132
6	4.4	28	1.788	5.256
7	4.4	28	1.823	5.359
8	4.4	28	1.775	5.169
9	4.4	28	1.794	5.204
10	4.4	45	1.489	3.935
11	5.5	15	2.730	7.369
12	5.5	40	1.770	4.272
13	6.0	28	2.223	5.413

Based on the analysis of variance, it was concluded that the 2-way interaction WFS·TS is not a significant term for the bead height model, as its P-value =0.061 is bigger than a significance level of α=0.05. That is why the 2-way interaction term was excluded from the model. Analysis of the bead width second-

order regression model shows that all the terms are significant and 2-factors interaction takes place.

For the CMT process, second order models were built for both ranges. Second-order models for range 1:

$$H_1 = 1.518 + 0.5407 \cdot WFS - 0.0574 \cdot TS$$
$$+ 0.001366 \cdot TS^2 - 0.0158 \cdot WFS \cdot TS \qquad (4)$$
$$W_1 = 1.82 + 4.102 \cdot WFS - 0.2269 \cdot TS - 0.395 \cdot WFS^2$$
$$+ 0.005151 \cdot TS^2 - 0.0421 \cdot WFS \cdot TS \qquad (5)$$

Second-order models for range 2:

$$H_2 = 2.653 + 0.1525 \cdot WFS - 0.08595 \cdot TS$$
$$+ 0.02302 \cdot WFS^2 + 0.001272 \cdot TS^2$$
$$- 0.004766 \cdot WFS \cdot TS \qquad (6)$$
$$W_2 = 3.554 + 2.3 \cdot WFS - 0.1887 \cdot TS - 0.1772 \cdot WFS^2$$
$$+ 0.002384 \cdot TS^2 - 0.01303 \cdot WFS \cdot TS \qquad (7)$$

Analysis of the variance for the CMT process showed that WFS^2 term is not significant for bead height determination in the first range, as its P-value=0.598 and was excluded from the model. For the conventional GMAW process, the maximal error does not exceed 4.75% for bead height and 6.57% for bead width. For the CMT process, the maximal error does not exceed 4.48% for bead height and 3.83% for bead width. Error (%E) was calculated as:

$$\%E = \frac{V_t - V_{exp}}{V_t} \cdot 100\% \qquad (8)$$

where V_t – theoretical value, V_{exp} – experimental value.

4. Validation and discussion

After determination of bead geometry, a few parts were produced by conventional GMAW (Figure 8a and Figure 9) and CMT WAAM (Figure 8b and Figure 10). To slice the CAD models, generate deposition paths and produce the parts with the required width, weld bead geometry was predicted with the help of the developed empirical equations described above.

Also, by using the response surface method, minimal and maximal values of bead height and width were determined (Table 5). Minimal values of bead geometry for the conventional GMAW process could be obtained with WFS 2.5 m/min and TS 56 cm/min. Maximal values with WFS 5 m/min and TS 15 cm/min. For the CMT process, minimal values correspond to WFS 1.2 m/min and TS 28 cm/min. Maximal values – WFS 6 m/min and TS 10 cm/min.

Table 5. Comparison of conventional GMAW and CMT processes.

Parameter	Process	
	Conventional	CMT
Minimal height, mm	1.14	1.098
Minimal width, mm	4.249	2.446
Maximal height, mm	2.596	3.374
Maximal width, mm	12.835	8.546
Maximal deposition rate, kg/h	1.55936	0.899627

Maximal deposition rate was calculated based on the area of

the maximal values of bead geometry. It was assumed that the cross section of the weld bead fit the parabola model. The area of the parabola function:

$$A = \frac{2}{3} H \cdot W \qquad (9)$$

where H – bead height [mm] and W – bead width [mm].

The deposition rate (DR) [kg/h] is calculated as:

$$DR = A \cdot \rho \cdot TS \cdot 10^{-8} \cdot 60 \qquad (10)$$

where A – cross section area of bead [mm^2], ρ – density of material [kg/m^3], TS – travel speed [cm/min].

Lower heat input (HI) during the CMT process leads to the lower deposition rate and significantly smaller bead widths compared to the conventional process. Thus, the CMT process benefits in production of thin-walled structures but requires more passes in case of thick-walled or solid components.

a)   b)

Figure 8 – Thin-walled part produced using a) conventional GMAW process; b) CMT process

Figure 9 - Thin walled vase with inclined walls produced using conventional GMAW process

Figure 10 – Thick-walled flange produced using CMT process

During the WAAM process heat loss decreases with the number of layers and leads to heat accumulation [9]. Heat accumulation causes variation of bead geometry, mainly increase of width and decrease of layer height. Due to reduced

layer height, the programmed Z height differs from the actual one. Thereby, contact tip to work distance (CTWD) increases from layer to layer, yielding current and voltage changes during the process and, as a result, variation of the bead geometry, poor gas shielding and porosities. That's why, to provide quality for the final part and stability of the process, temperature between the passes should be controlled by waiting for a certain amount of time between the layers or using in-situ cooling.

For the CMT process, the interpass time between the layers is lower compared to the conventional process, allowing to increase the welding time. The number of simultaneously produced parts also influences the productivity of the process. With an increasing number of parts, time that is spend for cooling of one piece has less influence on the total welding time.

In case of medium and large-scale parts, the conventional process could be preferable due to the resulting higher deposition rates. With increase of the part's scale, interlayer time could be decreased. If the scale of the part is large enough, then by the time the arc will come to the end point, the material at the start point will already have cooled down below the threshold value.

The complexity of the part also determines which process variant will be preferable. For the components that have simple geometries, both processes could be used. Geometries with overhanging features and inclined walls will significantly influence the process selection. As such, it is possible to produce thin-walls with a maximum inclination angle of 45˚ [10] with the conventional process using flat position deposition. Panchagnula et. al. [11] concluded that "for large overhangs, inclined slicing and 5-axis weld-deposition is often necessary". If the robot is used to implement the motion of the welding torch, a 2-axis rotary table is required, increasing the capital investment costs.

The CMT process provides more possibilities for deposition of inclined and vertical walls. Kazanas et.al. [12] reported that "wall type features could be added in any orientation from 0° to 180° without the use of support structures or the need to rotate the part.".

Comparison of the conventional and CMT processes showed that the choice of the process depends on the component size and the configuration and number of simultaneously produced parts.

5. Conclusion and future work

The main steps to be taken to adopt the existing GMAW technology combined with a standard welding robot for WAAM purposes were implemented. Experiments were conducted to build the empirical model for bead geometry prediction for both the conventional and CMT process. Results of experiments were verified by producing the parts. Comparison of the conventional and CMT processes showed that multiple factors such as the component size, configuration

and number of simultaneously produced parts, determine the applicability and productivity of the GMAW process.

However, the postprocessing step for the WAAM parts has not yet been investigated in detail and requires further work, also investigating the interaction between them. The amount of material that should be removed optimally during the subtractive manufacturing to provide the dimensional accuracy and surface quality of the final part should be determined.

Acknowledgements

References

[1] S. W. Williams, F. Martina, A. C. Addison, J. Ding, G. Pardal, and P. Colegrove, "Wire + Arc Additive Manufacturing," *Mater. Sci. Technol.*, vol. 32, no. 7, pp. 641–647, 2016.

[2] D. Ding, Z. Pan, D. Cuiuri, and H. Li, "Wire-feed additive manufacturing of metal components: technologies, developments and future interests," *Int. J. Adv. Manuf. Technol.*, vol. 81, no. 1–4, pp. 465–481, 2015.

[3] A. C. M. Bekker and J. C. Verlinden, "Life cycle assessment of wire + arc additive manufacturing compared to green sand casting and CNC milling in stainless steel," *J. Clean. Prod.*, vol. 177, pp. 438–447, 2018.

[4] A. Gomez Ortega, L. Corona Galvan, F. Deschaux-Beaume, B. Mezrag, and S. Rouquette, "Effect of process parameters on the quality of aluminium alloy Al5Si deposits in wire and arc additive manufacturing using a cold metal transfer process," *Sci. Technol. Weld. Join.*, vol. 23, no. 4, pp. 316–332, 2018.

[5] D. S. Nagesh and G. L. Datta, "Genetic algorithm for optimization of welding variables for height to width ratio and application of ANN for prediction of bead geometry for TIG welding process," *Appl. Soft Comput.*, vol. 10, no. 3, pp. 897–907, Jun. 2010.

[6] J. Xiong, G. Zhang, J. Hu, and L. Wu, "Bead geometry prediction for robotic GMAW-based rapid manufacturing through a neural network and a second-order regression analysis," *J. Intell. Manuf.*, vol. 25, no. 1, pp. 157–163, 2014.

[7] H. Geng, J. Xiong, D. Huang, X. Lin, and J. Li, "A prediction model of layer geometrical size in wire and arc additive manufacture using response surface methodology," *Int. J. Adv. Manuf. Technol.*, vol. 93, no. 1–4, pp. 175–186, 2017.

[8] D. C. Montgomery, G. C. Runger, and N. F. Hubele, *Engineering statistics, 5th Edition SI Version*. John Wiley & Sons, Inc., 2012.

[9] H. Zhao, G. Zhang, Z. Yin, and L. Wu, "A 3D dynamic analysis of thermal behavior during single-pass multi-layer weld-based rapid prototyping," *J. Mater. Process. Technol.*, vol. 211, no. 3, pp. 488–495, 2011.

[10] J. Xiong, Y. Lei, H. Chen, and G. Zhang, "Fabrication of inclined thin-walled parts in multi-layer single-pass GMAW-based additive manufacturing with flat position deposition," *J. Mater. Process. Technol.*, vol. 240, pp. 397–403, 2017.

[11] J. S. Panchagnula and S. Simhambhatla, "Manufacture of complex thin-walled metallic objects using weld-deposition based additive manufacturing," *Robot. Comput. Integr. Manuf.*, vol. 49, no. May 2017, pp. 194–203, 2018.

[12] P. Kazanas, P. Deherkar, P. Almeida, H. Lockett, and S. Williams, "Fabrication of geometrical features using wire and arc additive manufacture," *Proc. Inst. Mech. Eng. Part B J. Eng. Manuf.*, vol. 226, no. 6, pp. 1042–1051, 2012.